Drug-Delivery System Based on Core–Shell-Type Nanoparticles Composed of Poly(γ-benzyl-L-glutamate) and Poly(ethylene oxide)

JAE-WOON NAH,[1] YOUNG-IL JEONG,[2] CHONG-SU CHO[3], SUN-IL KIM[4]

[1] Department of Polymer Science and Engineering, Sunchon National University, Chonnam 540-742, South Korea

[2] Department of Polymer Engineering, Chonnam National University, Kwangju 500-757, South Korea

[3] Division of Biological Resources and Materials Engineering, Seoul National University, Suwon 441-744, South Korea

[4] Department of Chemical Engineering, Chonnam University, Kwangju 501-759, South Korea

Received 18 March 1999; accepted 27 July 1999

ABSTRACT: A block copolymer based on poly(γ-benzyl-L-glutamate) (PBLG) as the hydrophobic part and poly(ethylene oxide) (PEO) as the hydrophilic part was synthesized and characterized. PBLG/PEO/PBLG (GEG) block copolymer nanoparticles were prepared using the dialysis technique. Fluorescence spectroscopy measurement suggested that GEG block copolymers were associated in water to form polymeric micelles and the critical micelle concentration (CMC) value of the GEG-50 block copolymer was 0.0084 g/L. Particle-size distribution of the GEG-50 block copolymer based on the number average was 34.9 ± 17.6 nm. Also, the particle size and drug-loading contents of GEG nanoparticles were significantly changed with the initial solvent used. From transmission electron microscope (TEM) observations, the GEG polymeric micelle was a nice spherical shape and the sizes ranged from approximately 20–60 nm in diameter. Results from assessing the drug-loading contents against the initial solvent showed that the use of tetrahydrofuran (THF) or 1,4-dioxane as the initial solvent resulted in higher drug-loading contents than those of other solvents. In the drug-release studies, the higher the molecular weight of the polymer and drug-loading contents, the slower the drug release. Also, the initial solvent used was significantly affected not only in the drug-loading contents but also in the drug-release kinetics. © 2000 John Wiley & Sons, Inc. J Appl Polym Sci 75: 1115–1126, 2000

Key words: block copolymer; core-shell type nanoparticles; critical micelle concentration; drug delivery system; clonazepan

INTRODUCTION

Due to the ease of preparation and incorporation of bioactive agents, colloidal carriers or nanoparticles are extensively investigated for their potential for intravenous injection of drugs and for drug-targeting issues.[1–6] The potential of drug targeting to specific body sites would be of great benefit in the therapy of several diseases.[7–9] However, the potential of these colloidal carriers as drug-targeting systems are hampered by the clearance action of the reticuloendotheial system (RES), presenting a major obstacle in the use of such vehicles for site-specific drug delivery. Also, several problems may still exist such as the biodistribution of drugs, drug solubility, undesirable

Correspondence to: J.-W. Nah (jwnah@sunchon.ac.kr).

Contract grant sponsor: Korea Science and Engineering Foundation; contract grant number: 98-09-02-1.

Journal of Applied Polymer Science, Vol. 75, 1115–1126 (2000)

 CCC 0021-8995/00/091115-12

side effects, thermal instability, short blood circulation, structural fragility, and lower loading efficiency. To overcome these problems, several approaches have been attempted to attain effective site-specific drug delivery using novel carriers, such as surface-modified nanoparticles, liposomes, microspheres, polymeric micelles, and hydrophobized polysaccharides.[10–18]

Especially, core–shell-type nanoparticles or polymeric micelles formed in aqueous systems by self-assembly have attracted considerable attention in recent decades.[11,12,14,15,17,19,20] Due to their amphiphilic characteristics, block or graft copolymers, containing hydrophobic and hydrophilic components, exhibit surfactant behavior and form micelles or nanoparticles with a core–shell structure. In aqueous solutions, block or graft copolymers contain structures comprising hydrophobic cores surrounded by water-soluble polar groups which extend into the medium.[21] The block copolymers are known to form core–shell micellar structures at much lower values of critical micelle concentrations (CMC) than those from low molecular weight surfactants.[22] The block copolymer micelles are stable and dissociated slowly to free polymeric chains.[21–24] These drug-carrier systems with a core–shell structure have predominant characteristics, in that the hydrophobic inner core acts as a drug-incorporation site. This eases the entrapment of hydrophobic drugs by hydrophobic interactions,[25] and the hydrophilic outer shell may be cloaked to avoid being quickly taken up by the RES and clearable organs such as liver, spleen, lungs, and kidneys. They have the potential of long blood circulation times of polymeric carriers.[19] Some reported advantages of these systems include reduced toxic side effects of anticancer drugs, stable storage of the drug, long blood circulation, biodistribution, and lower interactions with the RES.[12,26]

In contrast to conventional microspheres or nanoparticles, core–shell-type nanoparticles or polymeric micelles have a generally reduced small particle size which is similar to natural biomolecule vehicles: viruses. Since the major factors to determine the fate of nanoparticulate carriers in the blood circulation is particle size and surface chemistry,[10,27,28] core–shell-type nanoparticles may be appropriate vehicles for drug delivery, such as an anticancer agent or other hydrophobic drugs. Thus, these drug carriers based on a core–shell structure may be selected for intravenous drug carriers as appropriate vehicles of site-specific targeting.

Langer et al.[11,17] reported that core–shell-type nanoparticles using a poly(lactide-*co*-glycolide)/poly(ethylene glycol) block copolymer, having been prepared in a one-step procedure, display increased blood circulation times compared to normal nanoparticles. Kataoka and collaborators[12,24,25] extensively investigated polymeric micelles as hydrophobic drug carriers such as for the anticancer agent Adriamycin. They reported that diblock copolymers composed of poly(β-benzyl-L-aspartate) (PBLA) and poly(ethylene oxide) (PEO) form micelles through self-association in water and have a several tens of nanometers, which is similar to the size range of viruses. They also reported enhanced tumor accumulation, long blood circulation times, and the effective treatment of solid tumors by the micelle-forming block copolymer–Adriamycin conjugate.[29,30]

Recently, we have been interested in the possibility of the formation of polymeric micelles based on a multiblock copolymer, little reported elsewhere. In previous studies, we reported on the formation of polymeric micelles of multiblock copolymers composed of poly(γ-benzyl-L-glutamate) (PBLG) and PEO and the potential of hydrophobic drug carriers.[15,31]

In this study, we synthesized the hexablock copolymer (abbreviated as GEG) composed of PBLG and PEO and prepared core–shell-type nanoparticles by a dialysis method. PBLG acts as the hydrophobic block which is the drug-incorporation site, the inner core, and has biodegradability.[32] PEO, as the outer shell, has a well-defined biocompatibility, is nontoxic, and has nonimmunogenic properties. It is known to avoid interaction with proteins and cells on the surfaces and interfaces.[33] Clonazepam (CNZ), as a model drug, is an anticonvulsant benzodiazepine, which is efficacious for the treatment of panic disorder and has a considerably hydrophobic character (water solubility < 14.66 μg drug/mL).[34,35] The physicochemical characteristics of GEG nanoparticles against the initial solvent used, drug-loading contents, and release characteristics were investigated.

EXPERIMENTAL

Materials

Bis[poly(ethylene oxide) bis(amine)] (BPEOBA: MW = 20,000) and PBLG were purchased from

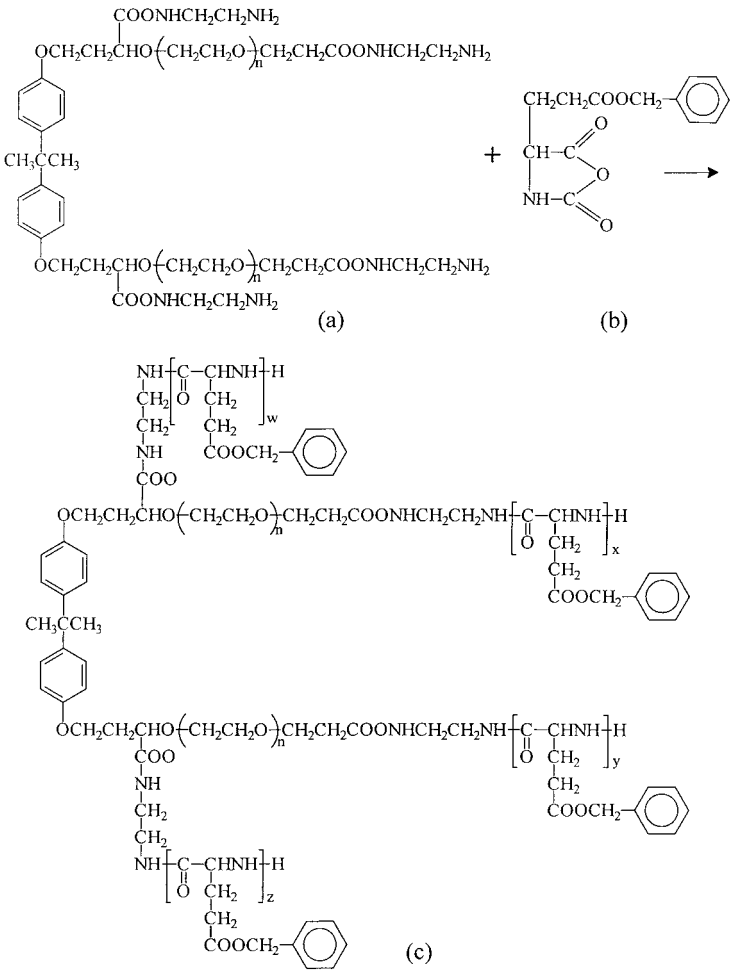

Figure 1 Synthesis scheme of GEG block copolymers.

the Sigma Chemical Co. (St. Louis, MO). The structure of BPEOBA is shown in Figure 1(a) according to the manufacturer's report. Triphosgene, *N*-hexane, and dichloromethane were purchased from the Aldrich Chemical Co. (Milwaukee, WI). All chemicals were used as reagent or spectrometric grade without further purification.

Synthesis of Block Copolymer

γ-Benzyl-L-glutamate *N*-carboxyanhydride (BLG–NCA) was prepared according to the method proposed by Goodman and Hutchison.[36] The block copolymer [Fig. 1(c)] was synthesized using a similar method reported previously.[15,31] The synthesis scheme is shown in Figure 1. In brief, the block copolymer was obtained by the polymerization of (b) BLG–NCA initiated by (a) the BPEOBA in dichloromethane, at a total concentration of BLG–NCA and BPEOBA of 3% (w/v), for 72 h at room temperature. The reaction progressed until the characteristic FTIR peak of BLG–NCA (1850, 1780, 915 cm^{-1}) disappeared. The reaction mixture was poured into a large excess of diethyl ether to precipitate the block copolymer. The reaction mixture may contain unreacted BPEOBA and block copolymers. Since BPEOBA cannot be precipitated from the mixture of dichloromethane and diethyl ether (although the latter is a nonsolvent for BPEOBA), the unreacted BPEOBA was removed by filtration with a glass filter and the block copolymer was obtained as precipitants. The resulting block copolymer was washed twice with diethyl ether and then dried *in vacuo* for 48 h.

Preparation of Core–Shell-type Nanoparticle

Polymeric micelles were prepared according to the previously reported method.[37,38] Twenty mil-

ligrams of the GEG block copolymer was dissolved in 5 mL of dimethylformamide (DMF) or other various solvents. The solution was stirred at room temperature and solubilized entirely. To form polymeric micelles, the solution was dialyzed using a molecular cutoff 12,000 g/mol dialysis tube against 1.0 L × 3 of distilled water for 3 h and then was distilled water-exchanged at intervals of 3–6 h for 2 days. The solution was then freeze-dried and stored at 4°C for the following analysis.

The formation of core–shell-type nanoparticles and the drug-loading procedure was carried out as follows: Thirty milligrams of the GEG block copolymer was dissolved in 7.5 mL of DMF or other various solvents and, subsequently, 15–30 mg of CNZ was added. The solution was then stirred until solubilized entirely at room temperature. To form nanoparticles and remove free drugs, the solution was dialyzed using a molecular cutoff 12,000 g/mol dialysis tube against 1.0 L × 3 of distilled water for 3 h and the water was exchanged at intervals of 3–4 h during a 24-h period. Then, the solution was freeze-dried. To evaluate the drug-loading content, a freeze-dried sample of GEG nanoparticles was suspended into methanol and vigorously stirred for 2 h and sonicated for 15 min. The resulting solution was centrifuged with 20,000 g for 30 min and the supernatant was taken for measurement of the drug concentration using a UV spectrophotometer (Shimadzu UV-1201) at 309 nm.

Nuclear Magnetic Resonance (NMR) Spectroscopy

^{1}H-NMR spectra of the copolymer for characterization of the GEG block copolymer was measured in $CDCl_3$ using a Bruker ARX-R300, 300-MHz NMR spectrometer.

Photon Correlation Spectroscopy (PCS) Measurements

PCS was measured with a Zetasizer 3000 (Malvern Instruments, England) with a He—Ne laser beam at a wavelength of 633 nm at 25°C (scattering angle of 90°). A nanoparticle solution prepared by the dialysis method was used for particle-size measurement (concentration: 0.1 wt %) and measured without filtering.

Observation of Transmission Electron Microscope (TEM)

The morphology of the polymeric micelles was observed using a TEM (JEOL, JEM-2000 FX II, Japan). A drop of a nanoparticle suspension in an aqueous solution was placed on a carbon film coated on a copper grid for TEM and freeze-dried. The specimen on the copper grid was not stained. Observation was done at 80 kV.

Measurement of Fluorescence Spectroscopy

To investigate the fluorescence spectroscopy characteristics, GEG block copolymer solutions were adjusted to the various concentrations of block copolymers. The CMC of the GEG block copolymers was estimated to prove the potential of micelle formation by the measurement of fluorescence spectroscopy (Shimadzu F-7000 spectrofluorometer, Shimadzu Co. Ltd., Tokyo, Japan) using pyrene as a probe.[22,39,40] To obtain sample solutions, a known amount of pyrene in acetone was added to each of a series of 20-mL vials and the acetone evaporated. The amount was adjusted to give a pyrene concentration in the final solution of $6.0 \times 10^{-7} M$. First, 10 mL of various concentrations of the block copolymer solutions were added to each vial, heated for 3 h at 65°C to equilibrate the pyrene and the micelles, and left to cool overnight at room temperature. For the fluorescence spectra, the excitation wavelength was 339 nm. The emission wavelength was 390 nm for the excitation spectra. Excitation and emission bandwidths were 1.5 and 1.5 nm, respectively.

In Vitro Release Studies

The release experiment *in vitro* was carried out as follows: Seven milligrams of CNZ-loaded nanoparticles and 1 mL phosphate-buffered saline (PBS, pH 7.4) were put into a dialysis tube. The dialysis tube was then introduced into a vial with 10 mL of PBS.[17,37] At specific time intervals, the whole medium was taken out and replaced with fresh PBS to prevent saturation of the drug. The concentration of the released CNZ was determined by a UV spectrophotometer (Shimadzu UV-1201) at 309 nm.

RESULTS AND DISCUSSION

GEG block copolymers prepared by the polymerization of γ-BLG NCA initiated with amine-terminated PEO in a methylene chloride solution are shown in Figure 1. It may be assumed that the polymerization mechanism is the primary amine

Table I Characterization of PBLG/PEO/PBLG Block Copolymers

Sample	Content of Monomeric Units (mol %)		
	PBLG	PEO[a]	$\overline{M_n}$
GEG-100	14.9	85.1	37,400
GEG-50	8.2	91.8	28,900
GEG-20	3.8	96.2	24,000

[a] MW of PEO: 20,000.

mechanism in which the initiator amine undergoes a nucleophilic addition to the C-5 carboxyl group of the NCA, as reported by Goodman and Hutchison.[36] Compositions and molecular weights of the copolymers are listed in Table I. The copolymer composition and the molecular weight were estimated from the peak intensities of the methylene proton signal (5.0 ppm) of the PBLG block and the methylene proton signal (3.7 ppm) of the PEO block in the NMR spectrum. Assuming that all the amine groups of the PEO participate in the polymerization, the number-average molecular weights, M_n, of the copolymer can be calculated from the copolymer composition and the molecular weight of the PEO chains.

Generally, AB-type diblock copolymers and ABA-type triblock copolymers exhibit micellar behavior in a selective solvent. For finite concentrations, larger than the CMC, the AB-type di- or ABA-type triblock copolymers associate into spherical micelles which consist of a meltlike inner core of insoluble B blocks and an exterior corona of soluble A blocks swollen by the solvent. On the other hand, BAB-type block copolymers also form micelles in the selective solvent.[41] Saito and Ishizu[41] reported that BAB-type block copolymers consisting of poly(2-vinylpyridine-*b*-styrene-*b*-2-vinylpyridine) form polymeric micelles in the selective solvent, which is good for A but not for B sequences, as in AB-type diblock copolymers. In this case, BAB-type block copolymers form flower-type or bridged flower-type polymeric micelles whose shells form a loop structure.[41–43] Also, differing from PEO-poly(propylene oxide) (PPO) or PEO–PPO–PEO, aqueous suspensions of reversed block copolymer architecture, PPO–PEO–PPO, display a rather different phase behavior.[42,44] But this system is also dominated by spherical micelles in a wide region of the phase diagram.[42] Mortensen[42] reported that aqueous solutions of PPO–PEO–PPO associate into a homogeneous phase constituting an interconnected network of micelles in which micellar cores of hydrophobic PPO are interconnected by hydrophilic PEO strands. Halperin[45] suggested that multiblock copolymers form molecular micelles, incorporating blocks belonging to a single copolymer. These molecular micelles composed of multiblock copolymers are expected to have a structurally similar architecture to BAB-type triblock copolymers in which coronal blocks form loops anchored to the inner core. In GEG block copolymers, which have a similar molecular architecture to the BAB-type triblock copolymer, and flower-type or bridged flower-type polymeric micelles in water are expected.

Wilhelm et al.[22] reported a micelle formation of polystyrene (PS) and PEO di- or triblock copolymers in water using a fluorescence technique with pyrene as a hydrophobic probe and determined the CMC from the fluorescence and excitation spectra, as pyrene partitions between aqueous and micellar environments. This method was also used by Kwon et al.[20] to approve the polymeric micelle formation of the PBLA and PEO diblock copolymer in water.

The formation of micelles was confirmed by a fluorescence-probe technique using pyrene as a

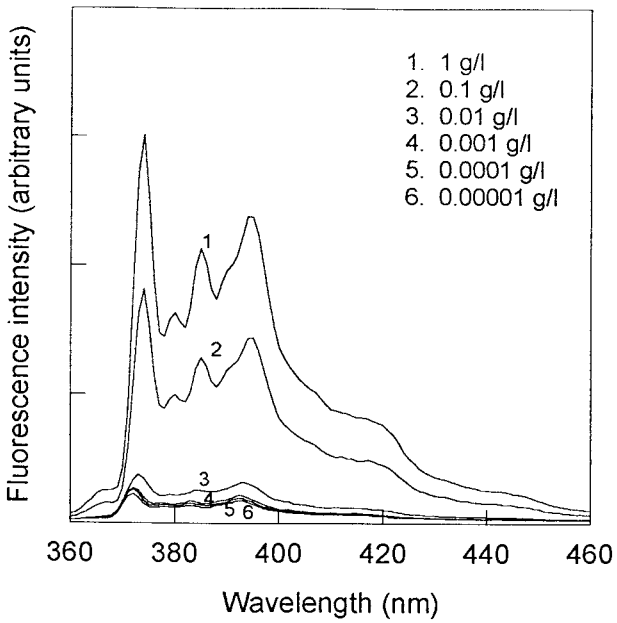

Figure 2 Fluorescence spectra of pyrene ($6.0 \times 10^{-7}M$)/GEG-50 against concentration of GEG-50 in distilled water. Excitation wavelength: 339.0 nm.

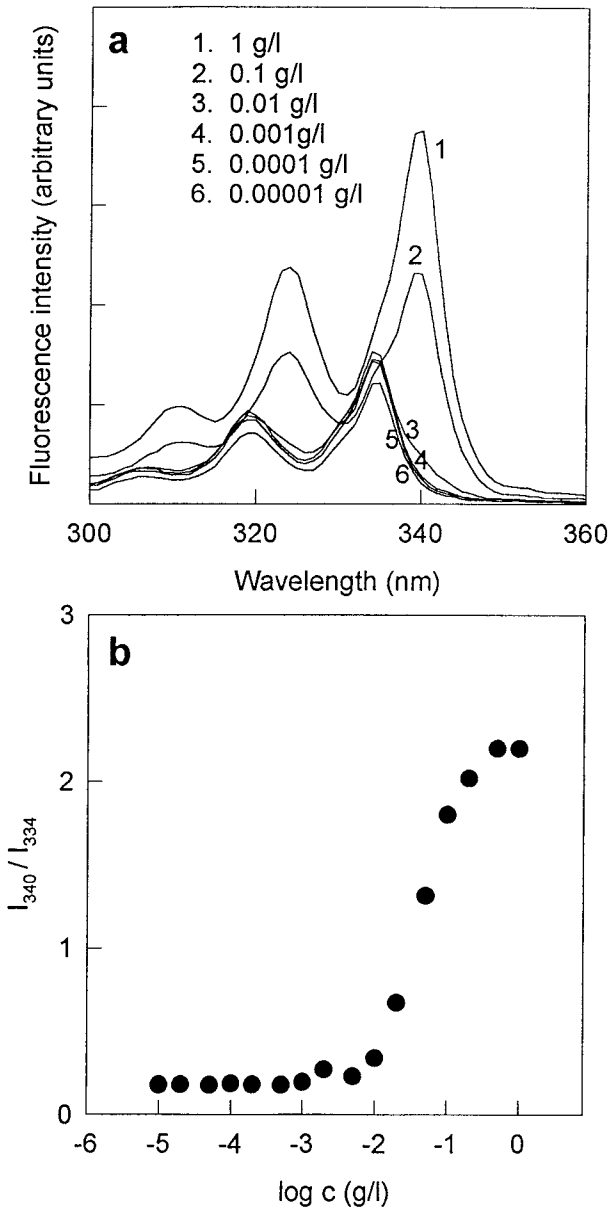

Figure 3 (a) Fluorescence excitation spectra of pyrene/GEG-50 against concentration of GEG-50 in distilled water. Emission wavelength: 390.0 nm. (b) Plot of the intensity ratio I_{339}/I_{334} from pyrene excitation spectra versus log c for block copolymers against concentration of GEG-2 in distilled water.

hydrophobic probe. Fluorescence spectra of GEG polymeric micelles at various concentrations in the presence of pyrene ($6.0 \times 10^{-7}M$) is shown in Figure 2. The spectrum is typical of pyrene fluorescence. Pyrene will be preferentially partitioned into hydrophobic cores with change to the photophysical properties of the molecules. The fluorescence intensity was increased and a change in the vibrational structure of the monomer fluorescence was observed with increasing concentrations of the GEG block copolymer.

Figure 3(a) shows the excitation spectrum of pyrene in the various concentrations of the GEG-50 block copolymer. In the excitation spectrum, a red shift was observed with increasing concentration of the GEG block copolymer. A red shift of pyrene in the excitation spectrum was observed in the study of micelle formation of the PS–PEO block copolymers.[22] The (0,0) bands in the pyrene excitation spectra were examined and compared with the intensity ratio I_{340}/I_{334}. This ratio takes the value characteristic of pyrene in water at low concentrations and the value of pyrene entirely in the hydrophobic domain. A plot of I_{340}/I_{334} versus log c is shown in Figure 3(b). A flat region in the low concentration extreme and sigmoidal region in the crossover region was noted. This result indicated that the signal change in the region of 0.0084 g/L ($2.9 \times 10^{-7}M$) can be evaluated as to the CMC values of the GEG block copolymer. As shown in Table II, the CMC values of the GEG block copolymer decreased with increase of the PBLG block chain length, that is, the shorter the PBLG chain length, the higher the CMC values. These results displayed similar tendencies to those reported previously.[14,15]

In the block copolymeric micelles, the block lengths and compositions of each of the segments affect the micellar properties such as the CMC, the micelle size, the aggregation number, the micelle stability, and the shape.[46,47] As the solvophobicity of the solvophobic part of the block copolymers increases, the CMC of the block copolymers decreases, and the average aggregation number and the size of the micelle is increased since the solvent repulsion force of the solvophobic block and the interfacial tension between the solvent and the surface of the micellar core increase.[46,47] Also, the selected solvent used to dissolve the block copolymer can be affected by the

Table II CMC Values for the GEG Block Copolymers by Fluorescence Spectroscopy Measurement

Sample	PBLG Contents (mol %)	CMC (mol)
GEG-100	14.9	2.1×10^{-7}
GEG-50	8.2	2.9×10^{-7}
GEG-20	3.8	8.3×10^{-7}

Table III Particle–size Distribution of GEG Block Copolymer Nanoparticles

	Particle Size (nm)		
Sample	Intensity Average	Volume Average	Number Average
GEG-100	142.8 ± 93.8	119.1 ± 67.4	106.5 ± 59.2
GEG-50	39.7 ± 19.7	37.4 ± 21.4	34.9 ± 17.6
GEG-20	18.2 ± 11.6	15.1 ± 4.3	13.5 ± 1.0

micellar properties described above due to the different polymer solubility in the solvent, difference of diffusion rate of the solvent into the aqueous environment, differences of each block of the copolymer in the solvent/water mixtures, and the solubility of the drug, etc.[48] These parameters also can be affect the particle size of the GEG block copolymer micelles.[49,50]

To confirm the nanoparticle formation of the GEG block copolymer, PCS and TEM was used to measure the particle size and morphological observations. The particle size of the GEG nanoparticles against the block copolymer composition is summarized in Table III. As shown in the results of the particle size of the GEG block copolymer, the larger the molecular weight of the GEG block copolymer, the bigger the particle size. These results indicated that the particle sizes were dependent on the molecular weight of the GEG block copolymer. In this result, the GEG nanoparticles have a small particle size without secondary aggregation as a monomodal distribution, which was typically observed in the di- or triblock copolymer micelles. Also, further investigations on the preparation of nanoparticles were performed using various solvents, because the selected initial solvent used to prepare the core–shell-type nanoparticles in water drastically affected the stability and particle size of the nanoparticles.[46]

Various solvents can be used in the preparation of nanoparticles. Among them, water-miscible solvents such as DMF, DMAc, DMSO, THF, and 1,4-dioxane were used to prepare the core–shell-type nanoparticles of the GEG block copolymers by the dialysis method. The effects of the initial solvent on the particle size of the GEG nanoparticles are summarized in Table IV. When DMF and DMAc as the initial solvent were used for the preparation of nanoparticles in water, particle sizes were relatively smaller than those of other solvents. In the study of polymeric micelles using PBLA and PEO diblock copolymers, La et al.[50] also reported that a small and narrow particle-size distribution was obtained using DMAc as the initial solvent for the preparation of polymeric micelles. But, in the case of DMF as the initial solvent for micelle formation, the results showed an increase in particle size and secondary aggregation which was different from our present result. Of course, a direct comparison cannot be made because different polymers and molecular architectures were used. The use of THF and 1,4-dioxane resulted in an increased particle size. Morphological observations of the GEG-50 block copolymer nanoparticles, prepared using DMF as the initial solvent, were performed using TEM without staining as shown in Figure 4. Their morphologies were nice spherical shapes and the sizes

Table IV Effect of Initial Solvent on the Particle Size of GEG-50 Block Copolymer

	Particle Size (nm)		
Solvent	Intensity Average	Volume Average	Number Average
DMF	39.7 ± 19.7	37.4 ± 21.4	34.9 ± 17.6
DMAc	22.6 ± 11.7	29.8 ± 19.1	20.3 ± 5.1
DMSO	56.8 ± 7.9	59.9 ± 11.3	56.6 ± 3.2
1,4-Dioxane	151.5 ± 21.2	150.7 ± 31.3	147.5 ± 27.1
THF	100.7 ± 13.8	110.1 ± 37.0	105.7 ± 25.2

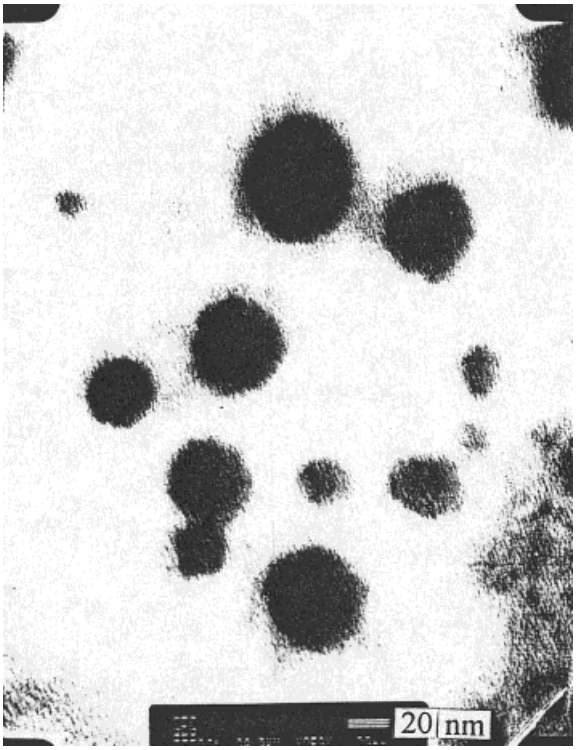

Figure 4 TEM photograph of GEG-50 block copolymer nanoparticles. Nanoparticles were prepared from DMF as the initial solvent.

ranged from about 20 to 60 nm, which were similar to the results of PCS. Interestingly, close observation of the TEM photographs revealed bright and dark images in the nanoparticles, demonstrating that the block copolymer showed core–shell-type nanoparticles. It seems that the dark part should be assigned to the core of the hydrophobic PBLG and the bright part should be assigned to the shell of the hydrophilic PEO. It can be said that the GEG block copolymeric nanoparticles prepared by the dialysis method have the potential of self-assembly to a hydrophobic-core and hydrophilic-outer-shell structure.

Further evidence of polymeric micelle formation of the GEG block copolymer and limited mobility of the PBLG chain in the core of the micelle was obtained with ^{1}H-NMR in $CDCl_3$ and D_2O (data not shown) in our previous ^{1}H-NMR studies.[51] Since both of the PBLG and PEO blocks dissolved easily in $CDCl_3$ or DMSO (*d*-form), micelle formation is not expected because of both blocks exist in the liquid state in that organic solvent. In $CDCl_3$ or DMSO (*d*-form), the characteristic peaks of the protons of the benzyl group and the methylene protons adjacent to the benzyl group of the PBLG segment were shown at 7.2–7.4 and 5.0–5.2 ppm, respectively (data not shown). Also, in that solvent, protons of the ethylene oxide of the PEO segment was shown at 3.6–3.7 ppm. But in D_2O, characteristic peaks of the PBLG block completely disappeared, whereas characteristic peaks of the PEO block remained. These results indicated that protons of the PBLG block display restricted motions within the micellar core and that the PBLG block has a rigid solid

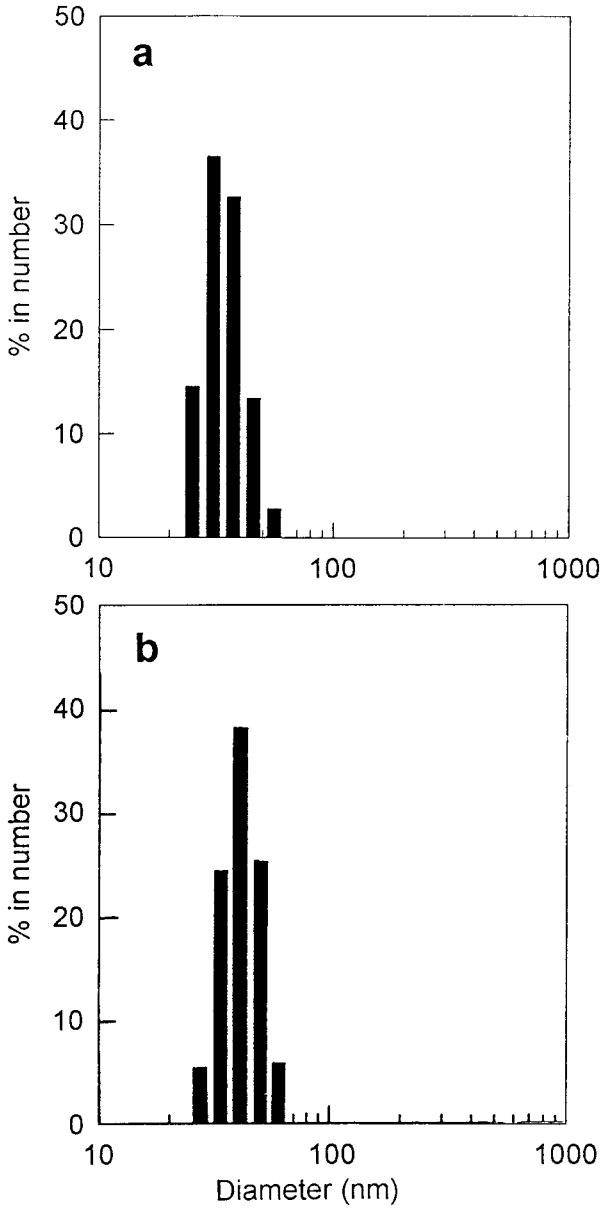

Figure 5 Particle-size distribution of GEG-50 block copolymers (a) without (b) and with drug loading (10.1 wt %) measured by photon correlation spectroscopy. Polymer concentration was 0.1 wt %.

Table V Effect of Polymer Composition and Initial Solvent on the Particle Size and Drug-loading Content of GEG Block Copolymeric Nanoparticles

Sample	Feeding Amount of Polymer (mg)	Feeding Amount of Drug (mg)	Initial Solvent[a]	Drug-loading Content (wt %)
GEG-100	30	15	DMF	8.3
GEG-50	30	30	DMF	10.1
	30	15	DMF	7.4
	30	30	DMAc	8.0
	30	30	THF	18.7
	30	30	1,4-Dioxane	23.8
	30	30	DMSO	10.3

[a] Volume of the initial solvent was 7.5 mL.

structure, whereas the PEO blocks existed as a liquid state in the aqueous environment. This behavior of the GEG micelles is in contrast to low molecular amphiphiles and the PEO–PPO–PEO block copolymers which typically exhibit liquid-like cores and relatively higher mobility. Kwon et al. also reported that the PBLA/PEO diblock copolymer has a rigid PBLA core.[20] But in their results, peaks of 7.4 and 5.2 ppm did not completely disappear and this result suggested that the PBLA/PEO diblock copolymer micelles may have a relatively less rigid core when compared with multiblock polymeric micelles.

Figure 5 shows the effect of drug loading on the particle-size distribution of the GEG block copolymer nanoparticles (prepared from DMF) based on the number average by PCS. The particle size of the GEG block copolymer without the drug [Fig. 5(a)] was 34.9 ± 17.6 based on the number average, but when the drug (10.1 wt %) was entrapped in the GEG block polymer nanoparticles [Fig. 5(b)], the particle size increased to 41.1 ± 21.3 nm. Table V shows the effect of the initial solvent on the drug-loading contents of the GEG block copolymer nanoparticles. When THF or 1,4-dioxane was used as the initial solvent, the drug-loading contents increased to higher than those of the other solvents. DMAc, as the initial solvent, resulted in the smallest drug-loading contents among them. When different amounts of the drug were supplied and the same solvent used, we observed that the higher the feeding amount of the drug, the more the drug-loading contents. Also, higher molecular weights of the block copolymer induced increased the drug-loading contents. From these results, it was indicated that the initial solvents used significantly affected the drug-loading contents.

To study the drug-release behavior, the CNZ-loaded nanoparticles of the GEG block copolymer against the block copolymer composition, drug-loading contents, and the initial solvents were simply redistributed in PBS (pH 7.4, 0.1*M*) and a drug-release study was performed *in vitro.* Figure 6 shows the release kinetics of CNZ from the nanoparticles of the GEG block copolymer as a function of the molecular weight of (a) the block copolymer and (b) the drug-loading contents. In the results of Figure 6(a), CNZ is continually released *in vitro* over 3 days (GEG-100) and 2 days (GEG-50) and the release pattern was revealed almost in a pseudo-zero-order kinetics. Although a direct comparison cannot be performed, the drug-release rate from the nanoparticles is relatively faster than that of the other microsphere systems because of the high surface area and small size of the nanoparticles. As shown in Figure 6(b), it was observed that the higher the drug-loading contents, the slower the drug release.

These phenomena were reported by several authors.[11,17,37,38] Gref et al.[11] reported that crystallization of a hydrophobic drug occurred inside the nanoparticles and that, especially at higher drug-loading contents in the nanoparticles, a phase separation occurs, leading to crystallization of part of the drug. Then, hydrophobic drugs loaded into nanoparticles release more slowly at higher drug loading contents, differing from hydrophilic water-soluble drugs. Also, our group observed that CNZ release had slower rate kinetics from the nanoparticles with higher drug-loading contents. On the other hand, at low drug loading, CNZ is relatively present as a molecular dispersion inside the nanoparticles.[11,17] The crystallized drug should dissolve and diffuse more slowly into the outer aqueous phase than in that of mo-

lecular dispersion. These characteristics of the drug-release behavior were supported by calorimetric analysis (data not shown) as reported previously.[37] Also, because of differences in the diffusivity of drug molecules to the outer aqueous phase, drug-release kinetics is affected not only by drug-loading contents but also by the size of the nanoparticles. For the same drug-loading contents, the drug-release rates in large nanoparticles were slower than in those of small-sized nanoparticles as reported elsewhere.[9]

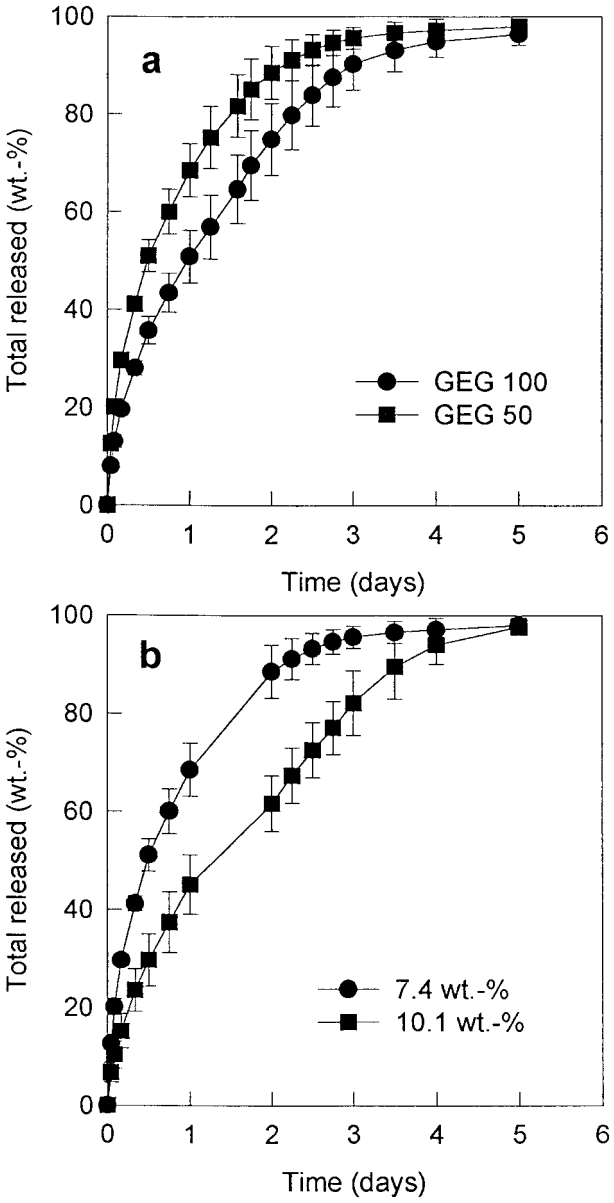

Figure 6 (a) CNZ release from core–shell-type nanoparticles of GEG-100 (drug-loading contents: 8.3 wt %) and GEG-50 (drug-loading contents: 7.4 wt %) and (b) against drug-loading contents.

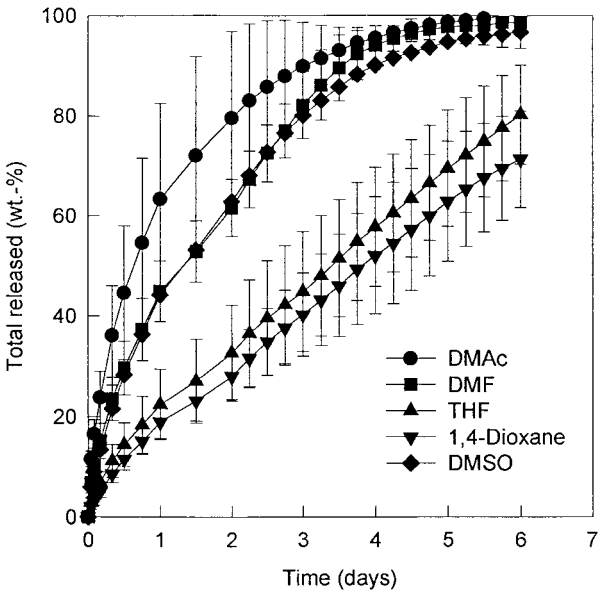

Figure 7 Effect of initial solvent on the release of clonazepam from core–shell-type nanoparticles. Drug-loading contents of each samples are described in Table V.

Figure 7 shows the CNZ release from the GEG block copolymer nanoparticles against the initial solvent used and the drug-loading contents were the same as described in Table V. As shown in Figure 7, the CNZ release rate in the case of DMAc, DMF, and DMSO was faster than that of THF and 1,4-dioxane. These results may be due to the differences of drug-loading contents against different initial solvents, which was similar with the above results of Figure 6. In the case of THF and 1,4-dioxane, the slower CNZ release rate might be due to the larger particle size and higher drug-loading contents. As a result, control of the drug-release kinetics can be achieved by optimizing the chemical nature of the used polymers, the drug-loading contents, and the particle size of the nanoparticles.

CONCLUSIONS

The block copolymer based on PBLG as the hydrophobic part and PEO as the hydrophilic part was synthesized and characterized. GEG block copolymer nanoparticles were prepared by a dialysis technique. The fluorescence spectroscopy measurement suggested that GEG block copolymers were associated in water to form polymeric micelles and the CMC value of the block copoly-

mer was 0.0084 g/L. The particle-size distribution of the GEG-2 block copolymer based on the number average was 34.9 ± 17.6 nm. Also, particle size and drug-loading contents of the GEG nanoparticles were significantly changed with the initial solvent used. From the TEM observations, the GEG polymeric micelle had a nice spherical shape and the sizes ranged from about 20–60 nm in diameter. Results from assessing the drug-loading contents against the initial solvents showed that the use of THF or 1,4-dioxane as the initial solvent resulted in higher drug-loading contents than that of the other solvents. In the drug-release studies, the higher the molecular weight of the polymer and drug-loading contents, the slower the drug release. Also, the initial solvent used was significantly affected, not only in drug-loading contents, but also in drug-release kinetics.

This work was supported by a grant from Korea Science and Engineering Foundation (98-09-02-1).

REFERENCES

1. Alleman, E.; Gurny, R.; Doelker, E. Eur J Pharm Biopharm 1993, 39, 173.
2. Choe, T.; Ku, J.; Jung, S.; Yang, J.; Kim, J. Kor J Chem Eng 1996, 13, 393.
3. Davis, S. S. Pharm Technol 1981, 5, 71.
4. Davis, S. S.; Illum, L.; Moghimi, S. M.; Davies, M. C.; Porter, C. J. H.; Muir, I. S.; Brindley, A.; Christy, N. M.; Norman, M. E.; Williams, P.; Dunn, S. E. J Control Rel 1993, 24, 157.
5. Kreuter, J. J Control Rel 1993, 16, 169.
6. Yoshioka, T.; Hashida, M.; Muranishi, S.; Sezaki, H. Int J Pharm 1981, 81, 131.
7. Couvreur, P.; Fattal, E.; Andremont, A. Pharm Res 1991, 8, 1079.
8. Couvreur, P.; Fattal, E.; Alphandary, H.; Puisieux, F.; Andremont, A. J Control Rel 1992, 19, 259.
9. Leroux, J. C.; Allemann, E.; Jaeghere, F. D.; Doelker, E.; Gurny, R. J Control Rel 1996, 39, 339.
10. Dunn, S. E.; Brindley, A.; Davis, S. S.; Davies, M. C.; Illum, L. Pharm Res 1994, 11, 1016.
11. Gref, R.; Minamitake, Y.; Peracchia, M. T.; Trubetskoy, V.; Torchilin, V.; Langer, R. Science 1994, 263, 1600.
12. Kataoka, K.; Kwon, G. S.; Yokoyama, M.; Okano, T.; Sakurai, Y. J Control Rel 1993, 24, 119.
13. Lasic, D. D. Nature 1992, 355, 279.
14. Nah, J. W.; Jeong, Y. I.; Cho, C. S. J Polym Sci B Polym Phys 1998, 36, 415.
15. Nah, J. W.; Jeong, Y. I.; Cho, C. S. Bull Kor Chem Soc 1998, 19, 962.
16. Nah, J. W.; Lee, D. B.; Cho, C. S.; Jeong, Y. I.; Kim, S. H.; Kim, S. H. J Kor Chem Soc 1998, 42, 92.
17. Peracchia, M. T.; Gref, R.; Minamitake, Y.; Domb, A.; Lotan, N.; Langer, R. J Control Rel 1997, 46, 223.
18. Scholes, P. D.; Coombes, A. G. A.; Illum, L.; Davis, S. S.; Vert, M.; Davies, M. C. J Control Rel 1993, 25, 145.
19. Kwon, G. S.; Yokoyama, M.; Okano, T.; Sakurai, Y.; Kataoka, K. Pharm Res 1993, 11, 970.
20. Kwon, G. S.; Naito, M.; Yokohama, M.; Okano, T.; Sakurai, Y.; Kataoka, K. Langmuir 1993, 9, 945.
21. Brown, W.; Schillen, K.; Almgren, M.; Hvidt, S.; Bahadur, P. J Phys Chem 1991, 95, 1850.
22. Wilhelm, M.; Zhao, C. L.; Wang, Y.; Xu, R.; Winnik, M. A.; Mura, J. L.; Riess, G.; Croucher, M. D. Macromolecules 1991, 24, 1033.
23. Malmsten, M.; Lindman, B. Macromolecules 1992, 25, 5440.
24. Yokoyama, M.; Miyauchi, M.; Yamada, N.; Okano, T.; Sakurai, Y.; Kataoka, K.; Inoue, S. J Control Rel 1990, 11, 269.
25. Kwon, G. S.; Naito, M.; Yokoyama, M.; Okano, T.; Sakurai, Y.; Kataoka, K. Pharm Res 1995, 12, 192.
26. Kwon, G.; Suwa, S.; Yokoyama, M.; Okano, T.; Sakurai, Y.; Kataoka, K. J Control Rel 1994, 29, 17.
27. Illum, L.; Davis, S. S.; Wilson, C. G.; Frier, M.; Hardy, J. G.; Thomas, N. W. Int J Pharm 1982, 12, 135.
28. Illum, L.; Hunneyball, I. M.; Davis, S. S. Int J Pharm 1986, 29, 53.
29. Yokoyama, M.; Miyauchi, M.; Yamada, N.; Okano, T.; Sakurai, Y.; Kataoka, K.; Inoue, S. Cancer Res 1990, 50, 1693.
30. Yokoyama, M.; Okano, T.; Sakurai, Y.; Ekimoto, H.; Shibazaki, C.; Kataoka, K. Cancer Res 1991, 51, 3229.
31. Cho, C. S.; Na, J. W.; Jeong, Y. I.; Kim, S. H.; Lee, Y. M.; Sung, Y. K. Polymer (Kor) 1995, 19, 926.
32. Cho, C. S.; Kim, S. U. J Control Rel 1988, 7, 283.
33. Lee, J. H.; Kopecek, J.; Andrade, J. D. J Biomed Mater Res 1989, 23, 351.
34. Mura, P.; Liguori, A.; Bramanti, G.; Corti, P.; Murratzu, C.; Celesti, L. Pharm Acta Helv 1990, 65, 298–303.
35. White, H. S. In Remington: The Science and Practice of Pharmacy, 19th ed.; Gennaro, A. R., Eds.; Mack: Easton, PA, 1995; Vol. 2, pp 1173–1174.
36. Goodman, M.; Hutchison, J. J Am Chem Soc 1966, 88, 3627.
37. Jeong, Y. I.; Cheon, J. B.; Kim, S. H.; Nah, J. W.; Lee, Y. M.; Sung, Y. K.; Akaike, T.; Cho, C. S. J Control Rel 1998, 51, 169.
38. Kim, H. J.; Jeong, Y. I.; Kim, S. H.; Lee, Y. M.; Cho, C. S. Arch Pharm Res 1997, 20, 324.

39. Kalyanasundaram, K.; Thomas, J. K. J Am Chem Soc 1977, 99, 2039.
40. Marctic, P. A.; Nair, M. J Colloid Interf Sci 1994, 163, 517.
41. Saito, R.; Ishizu, K. Polymer 1997, 38, 225.
42. Mortensen, K.; Brown, W.; Jorgensen, E. Macromolecules 1994, 27, 5654.
43. Mortensen, K. Macromolecules 1997, 30, 503–507.
44. Mortensen, K.; Pedersen, J. S. Macromolecules 1993, 26, 805.
45. Halperin, A. Macromolecules 1991, 24, 1418.
46. Whitmore, M. D.; Noolandi, J. Macromolecules 1985, 18, 657.
47. Nagarajan, R.; Ganesh, K. J Phys Chem 1989, 90, 5843.
48. Bodmeier, R.; McGinity, J. W. Int J Pharm 1988, 43, 179.
49. Cheon, J. B.; Jeong, Y. I.; Cho, C. S. Polymer 1999, 40, 2041.
50. La, S. B.; Okano, T.; Kataoka, K. J Pharm Sci 1996, 85, 85.
51. Nah, J. W.; Jeong, Y. I.; Cho, C. S. Bull Kor Chem Soc in press.